Electrochemical Reduction of Carbon Dioxide Using Iron-Sulfur Clusters as Catalyst Precursors

Makoto NAKAZAWA, Yasushi MIZOBE, Yoichi MATSUMOTO,† Yasuzo UCHIDA,†
Meguru TEZUKA,†† and Masanobu HIDAI*
Engineering Research Institute, Faculty of Engineering, The University of Tokyo,
Yayoi, Bunkyo-ku, Tokyo 113
†Department of Industrial Chemistry, Faculty of Engineering, The University of Tokyo,
Hongo, Bunkyo-ku, Tokyo 113
††The Saitama Institute of Technology, Okabe, Saitama 369-02
(Received, September 24, 1985)

The potential-current relationships of DMF solutions of a series of iron-sulfur compounds have revealed that in the presence of clusters $[Fe_4S_4(SR)_4]^{2-}$ (R=$PhCH_2$ or Bu^t) and $[M_2Fe_6S_8(SEt)_9]^{3-}$ (M=Mo or W) the electroreduction of CO_2 proceeds at the potential shifted by about 0.7 and 0.5 V, respectively, to the positive direction compared to the potential at which CO_2 is reduced without any catalyst. When controlled potential electrolysis of a DMF solution containing $[Fe_4S_4(SCH_2Ph)_4]^{2-}$ was carried out under CO_2 at −2.0 V vs. SCE, phenylacetate and formate were formed as the products resulting from CO_2 reduction. The cubane structure of this cluster collapsed rapidly under these conditions. However, when excess amount of $PhCH_2SH$ was added to the catholyte, the cluster structure was preserved during a relatively long period of electrolysis, and the yield of phenylacetate increased but that of formate decreased compared with the reaction in the absence of free $PhCH_2SH$.

Utilization of carbon dioxide has evoked much interest in relevance to the development of alternative carbon sources of fuels and chemicals. However, the fixation of CO_2, the stable carbon end product, inevitably necessitates considerable energy input. The electrochemical reduction of CO_2 is presumably one of the most potential methods for converting CO_2 into organic substances but the direct reduction requires the large overpotential.[1-4] Recently several transition metal complexes were reported as the catalysts to diminish the overvoltage. Among these are Co and Ni tetraazamacrocycles,[5-9] [Re(bipyridine)$(CO)_3Cl$][10] and [Rh(diphosphine)$_2$Cl].[11] From the former two catalytic systems, CO is produced in high current efficiencies, whereas the Rh complex catalyzes the formation of formate. In a previous communication, we reported that the iron-sulfur clusters $[Fe_4S_4(SR)_4]^{2-}$([2−]), first prepared by Holm and his coworkers as the ferredoxin model compounds,[12] remarkably diminish the overvoltage of CO_2 electroreduction.[13] From this reaction system, a substantial amount of formate is obtained together with a little CO. Here we wish to describe the detail of this reaction.

Results and Discussion

Current-Potential Relationships of DMF Solutions Containing Iron-Sulfur Clusters under CO_2. The direct electroreduction of CO_2 in nonaqueous media has been reported by several authors.[3,14] In every case the reduction proceeds only at extremely negative potentials. In fact, investigation of the reduction of CO_2 in a solution of 0.1 M $[Bu^n_4N][BF_4]$ (M= mol dm^{-3}) in DMF on mercury electrode has revealed that potentials more negative than −2.4 V vs. SCE are required for the reduction. However, addition of 2 mM $[Fe_4S_4(SR)_4]^{2-}$ (R=CH_2Ph or Bu^t) to the solution lowers the effective reduction potential by about 0.7 V. Figure 1 shows the current (I)-potential (E) relationship of a solution of $[Fe_4S_4(SCH_2Ph)_4]^{2-}$ (**1**) in DMF recorded on mercury pool cathode with 13.5 cm^2 surface area. Cluster **1** exhibits two succesive reduction waves corresponding to two redox processes [2−]/[3−] and [3−]/[4−] under N_2 (Fig. 1 c). When CO_2 gas was bubbled

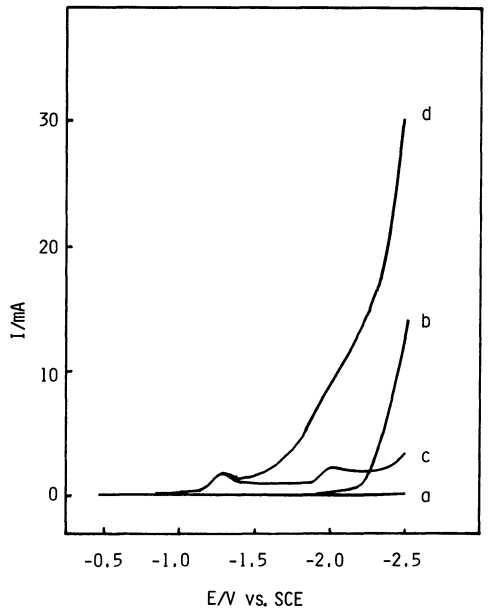

Fig. 1. I–E relationships of a solution of 0.1 M $[Bu^n_4N][BF_4]$ in DMF. (a): Without cluster under N_2, (b): Without cluster under CO_2, (c): In the presence of 2 mM cluster **1** under N_2, (d): In the presence of 2 mM cluster **1** under CO_2.

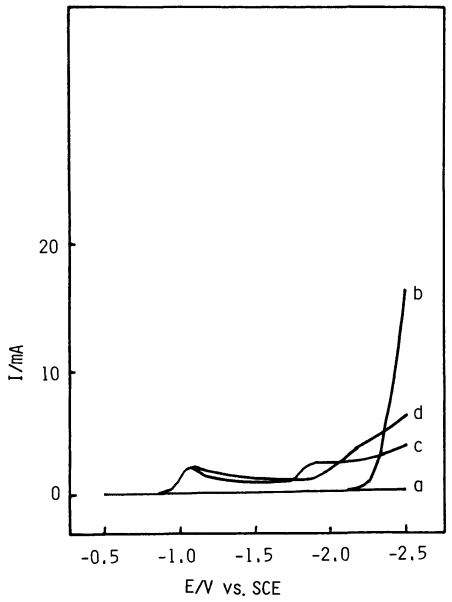

Fig. 2. *I–E* relationships of a solution of 0.1 M $[Bu^n_4N][BF_4]$ in DMF. (a): Without cluster under N_2, (b): Without cluster under CO_2, (c): In the presence of 2 mM cluster **3** under N_2, (d): In the presence of 2 mM cluster **3** under CO_2.

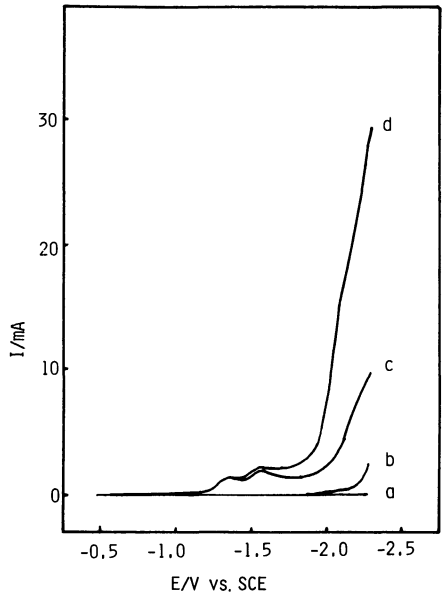

Fig. 3. *I–E* relationships of a solution of 0.1 M $[Bu^n_4N][BF_4]$ in DMF. (a): Without cluster under N_2, (b): Without cluster under CO_2, (c): In the presence of 2 mM cluster **4** under N_2, (d): In the presence of 2 mM cluster **4** under CO_2.

through the solution for several minutes, the reduction current of CO_2 increased remarkably at potentials more negative than −1.7 V (Fig. 1 d). The same trend is also observed in the case of $[Fe_4S_4(SBu^t)_4]^{2-}$ (**2**). In contrast with these compounds, the cluster $[Fe_4S_4(SPh)_4]^{2-}$ (**3**) does not have any effect on the electroreduction of CO_2 as shown in Fig. 2. Although cluster **3** is reduced to [3−] and then [4−] in the same manner as clusters **1** and **2**, the electron transfer from the reduced **3** to CO_2 does not occur substantially. When cluster **1** was reduced to [4−] under CO_2, it decomposed rapidly to generate in situ the other species which enhanced the electroreduction of CO_2 (vide infra). On the other hand, degradation of cluster **3** also proceeded substantially under the same conditions but the similar enhancement for reduction of CO_2 was not observed. It is interesting that the rate of the electroreduction of CO_2 depends very much upon the kind of thiolate ligands of cluster [2−].

We have also examined the potential-current relationships of DMF solutions of a series of other iron-sulfur compounds under N_2 and CO_2. The molybdenum-iron-sulfur cluster $[Mo_2Fe_6S_8(SEt)_9]^{3-}$ (**4**) is effective for the reduction of CO_2 (Fig. 3). The positive shift of the reduction potential amounts to about 0.5 V. The tungsten analogue $[W_2Fe_6S_8(SEt)_9]^{3-}$ also gives essentially the same results. However, the analogous clusters containing SPh ligands cannot facilitate the electroreduction of CO_2, as is also observed for cluster **3** (Fig. 4). The mononuclear

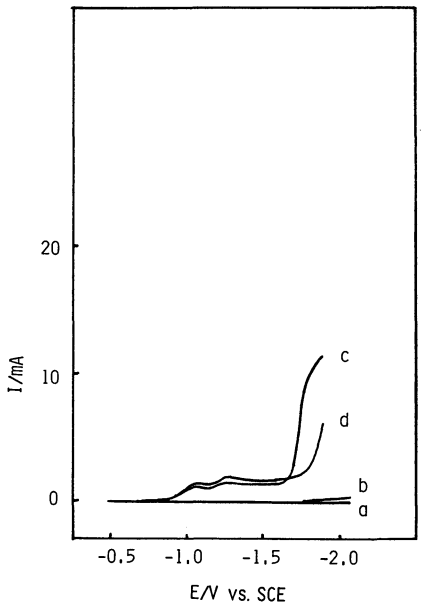

Fig. 4. *I–E* relationships of a solution of 0.1 M $[Bu^n_4N][BF_4]$ in DMF. (a): Without cluster under N_2, (b): Without cluster under CO_2, (c): In the presence of 2 mM cluster **5** under N_2, (d): In the presence of 2 mM cluster **5** under CO_2.

compound $[Fe(SEt)_4]^{2-}$ decomposed immediately in DMF to give an insoluble solid, when CO_2 was bubbled through the solution, and the *I–E* curve of this mixture under CO_2 is just the same as that of the direct noncatalyzed reduction. On the other hand,

the dinuclear compound $[Fe_2S_2(SEt)_4]^{2-}$ was rapidly converted to the cubane cluster with Fe_4S_4 core under the electrolytic condition.[15] Therefore, the *I–E* curve of a solution of this cluster in DMF becomes very close to that of cluster [2−].

Controlled Potential Electrolysis of a Solution of $[Fe_4S_4(SCH_2Ph)_4]^{2-}$ (1) or $[Mo_2Fe_6S_8(SEt)_9]^{3-}$ (4) in DMF Saturated with CO_2. Since a DMF solution of cluster **1** has demonstrated an excellent CO_2 fixing ability under the electroreductive conditions, the preparative controlled potential electrolysis was performed at the potential of −2.0 V vs. SCE by using $[Bu^n_4N][BF_4]$ as suporting electrolyte. Since CO was produced only with 1—2% current efficiency from the present system as reported already,[13] the analysis of the gaseous phase was omitted hereafter and CO_2 was bubbled through the catholyte during electrolysis to enhance the reaction rate.

To determine the lifetime of cluster **1** as catalyst, time-dependence of the concentration of cluster **1** during the electrolysis has been followed by measuring the cyclic voltammograms and the absorption spectra of the reaction solution, which are shown in Fig. 5. In the cyclic voltammograms, the reduction wave at the peak potential of about −1.4 V corresponding to the [2−]→[3−] process is observed clearly at the early stage of the electrolysis but it disappears when the electrolysis is furthermore continued. The absorption spectra of the catholyte also show a rapid decrease of the absorption band at 420 nm characteristic of cluster **1**. These findings indicate that the cubane structure of cluster **1** is preserved only for an initial period and CO_2 fixation catalyzed by cluster **1** occurs only at the early stage. However, it should be noted that the reduction current observed at potentials more negative than −1.5 V increases remarkably after the degradation of the cubane structure. This implies that other type(s) of catalysts may be generated in situ. Analogous rapid decomposition of the cubane structure is also observed when a DMF solution containing molybdenum-iron-sulfur cluster **4** is electrolyzed at −2.0 V under CO_2.

The products in the catholyte were analyzed by HPLC after removing the solid deposited by the addition of water to the electrolyte. A typical liquid chromatogram of the catholyte obtained from the electrolysis of the system containing cluster **1** is given in Fig. 6, which indicates the formation of six products (A—F). None of these peaks appeared in the chromatogram of the catholyte if the reduction was carried out at −2.0 V in the absence of cluster **1**. Formate corresponds to peak B. No oxalate was produced in this catalytic electrolysis. This is in sharp contrast to the predominant formation of oxalate in the electrolysis of CO_2 at −2.4 V in DMF without any catalyst. The product A isolated by preparative HPLC was identified as phenylacetate by its IR and NMR spectra. Isolation of the other products C, D, and E was also attempted. Since the IR spectra of these products in crude forms do not show C=O stretching bands, these compounds are

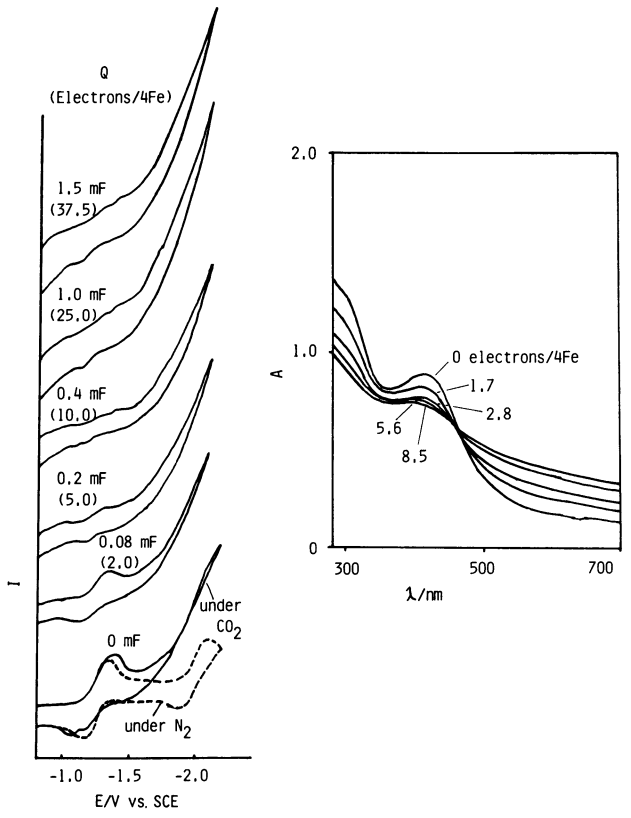

Fig. 5. Dependence of cyclic voltammograms (left) and absorption spectra (right) of a solution of 2 mM cluster 1 in DMF on the electricities passed.

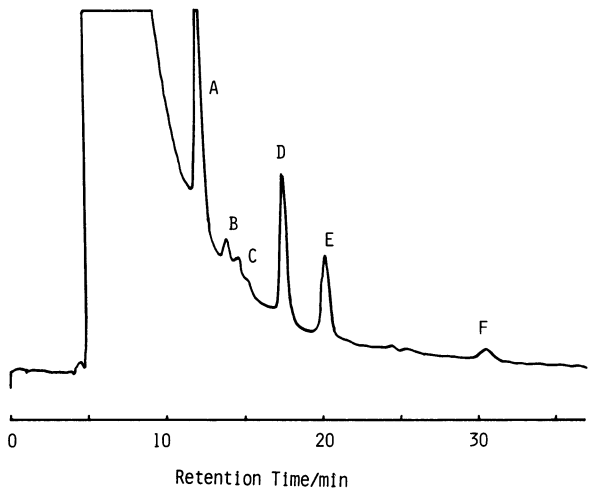

Fig. 6. Liquid chromatogram of the products after the electrolysis in the presence of 2 mM cluster **1** until 1.5 mF of electricities passed.

probably not derived from the electroreduction of CO_2. Thus, more effort to characterize these compounds was abandoned.

When the electrolysis of a DMF solution containing cluster **4** was performed at −2.0 V vs. SCE under CO_2, three products were detected by the HPLC analysis of the catholyte. One of them could be assigned to formate but the yield was quite low. The IR spectra of the other two components in crude forms indicate that these products may not be derived from CO_2. Neither propionate, which may be expected on the analogy of the formation of phenylacetate from the system containing **1**, nor oxalate was produced.

Table 1. Yields of Phenylacetate and Formate Formed by the Controlled Potential Electrolysis Using Cluster **1** as Catalyst Precursor[a)]

Q/mF	Phenylacetate Yield mol/4Fe atoms	Phenylacetate η %	Formate Yield mol/4Fe atoms	Formate η %
0.5	0.40	6.4	0.85	14
1.0	0.50	4.2	2.4	19
1.5	0.58	2.8	3.3	17
2.0	0.68	2.7	5.5	22
3.0	0.75	2.0	10	27
4.0	0.88	1.8	10	20
5.0	0.88	1.4	11	17

a) Cluster **1**: 2 mM; $[Bu^n_4N][BF_4]$: 0.1 M; At −2.0 V vs. SCE.

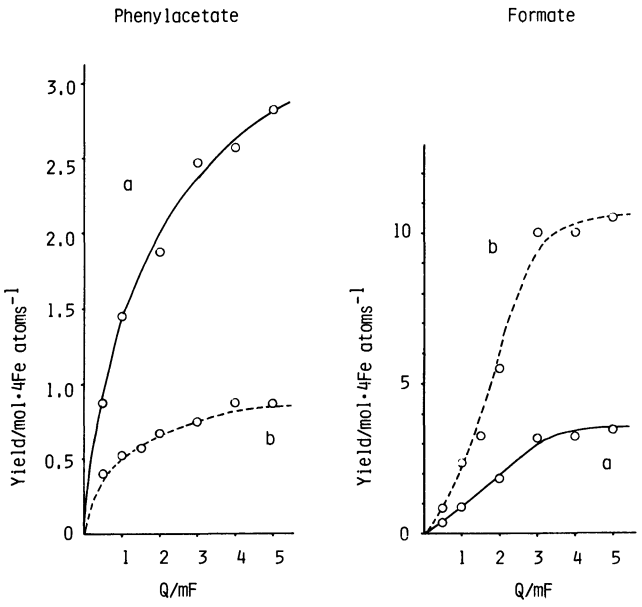

Fig. 7. Yields of phenylacetate and formate formed by the electrolysis of a solution of 2 mM cluster **1** in the presence (full line) or absence (broken line) of excess $PhCH_2SH$.

Formation of Phenylacetate and Formate by Controlled Potential Electrolysis Catalyzed by Cluster 1. In Table 1 are summarized the yields of phenylacetate and formate when the electroreduction of CO_2 in the presence of cluster **1** was continued until the prescribed electricities passed. Current efficiencies (η) are calculated by assuming that two electrons are required in the formations of each product ($H^+ + CO_2 + 2e^- \rightarrow HCOO^-$, $PhCH_2S^- + CO_2 + 2e^- \rightarrow PhCH_2COO^- + S^{2-}$).

The yields of these products are visuallized in Fig. 7 by broken lines. Production of both compounds nearly finished when about 3 mF of electricities passed. The ultimate yield of phenylacetate is close to 1 mol per mol of cluster **1** initially added to the catholyte before the electrolysis. This suggests that phenylacetate is produced from one thiolate ligand of each cubane. Degradation of the cubane structure, which is monitored by the change of cyclic voltammograms and absorption spectra of the reaction mixture, is probably initiated by the conversion of one $PhCH_2S$ ligand into phenylacetate. The final yield of formate amounts to about 10 mol per mol of cluster **1** in the catholyte for the electrolysis continued until 3 mF or more electricities have passed. The optimum current efficiency of 27% for production of formate is observed when 3.0 mF of electricities have passed. The hydrogen atom in formate, at least in part, seems to be derived from tetraalkylammonium ion of the supporting electrolyte or the cation of cluster **1**, since in the gas analysis after the electrolysis were detected considerable amounts of hydrocarbons, which were undetectable in such cases where oxalate was formed predominantly.

Since the conversion of $PhCH_2S$ ligands of cluster **1** into phenylacetate proceeds under this electrolytic conditions concurrent with the collapse of the cubane core, excess $PhCH_2SH$ was added to the catholyte to retain the cubane structure. Table 2 and the full line

Table 2. Yields of Phenylacetate and Formate Formed by the Electrolysis in the Presence of Excess $PhCH_2SH$[a)]

Q/mF	Phenylacetate Yield mol/4Fe atoms	Phenylacetate η %	Formate Yield mol/4Fe atoms	Formate η %
0.5	0.88	14	0.35	5.6
1.0	1.5	12	0.85	6.8
2.0	1.9	7.5	1.8	7.3
3.0	2.5	6.6	3.2	8.5
4.0	2.6	5.2	3.3	6.5
5.0	2.8	4.5	3.5	5.6

a) Cluster **1**: 2 mM; $[Bu^n_4N][BF_4]$: 0.1 M; $PhCH_2SH$: 21 mol/4Fe atoms; At −2.0 V vs. SCE.

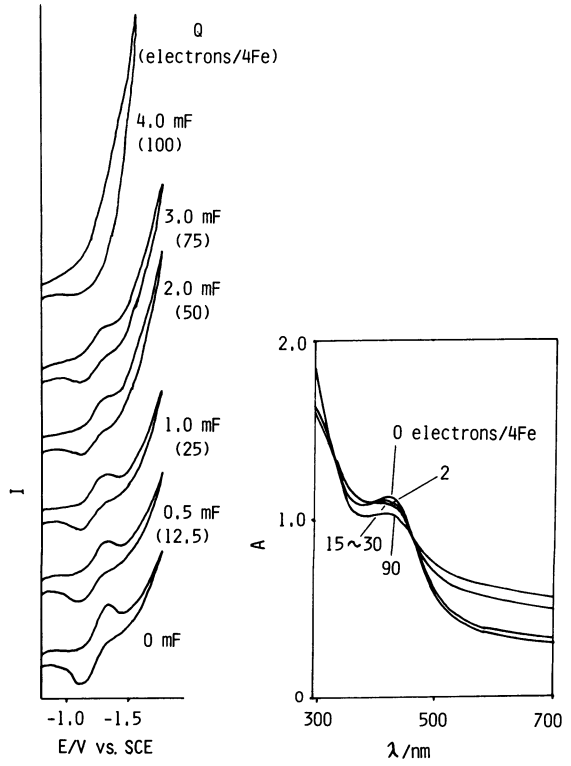

Fig. 8. Dependence of cyclic voltammograms (left) and absorption spectra (right) of a solution of 2 mM cluster **1** in DMF on the electricities passed in the presence of excess $PhCH_2SH$.

in Fig. 7 show the yields of phenylacetate and formate when the electrolysis was carried out in the presence of excess $PhCH_2SH$ (21 mol/mol of cluster **1**). The yield of phenylacetate is approximately tripled compared to that from the original system, whereas the formation of formate is remarkably supressed. Figure 8 illustrates time dependence of cyclic voltammograms and absorption spectra taken during the electrolysis, which definitely shows the retention of the redox wave and the absorption band characteristic of cluster **1**. This indicates that addition of excess $PhCH_2SH$ to the catholyte can prevent degradation of the cluster structure. Since the yield of formate decreases while the cluster structure is maintained, the species that catalyze the formation of formate are not the reduced cluster **1** but the other stuff generated in situ from cluster **1**.

Experimental

Materials. Iron-sulfur compounds, $[Et_4N]_2[Fe_4S_4(SCH_2Ph)_4]$(**1**),[12] $[Me_4N]_2[Fe_4S_4(SBu^t)_4]$(**2**),[12,16] $[Bu^n{}_4N]_2[Fe_4S_4(SPh)_4]$ (**3**),[12] $[Et_4N]_3[Mo_2Fe_6S_8(SEt)_9]$(**4**),[17,18] $[Bu^n{}_4N]_3[Mo_2Fe_6S_8(SPh)_9]$(**5**),[17] $[Et_4N]_3[W_2Fe_6S_8(SEt)_9]$,[17] $[Me_3NCH_2Ph]_2[Fe(SEt)_4]$,[19] and $[Me_3NCH_2Ph]_2[Fe_2S_2(SEt)_4]$[19] were prepared according to the published methods and handled under a nitrogen atmosphere. DMF was dried over CaH_2 and distilled under reduced pressure of N_2 before use.

Electrochemical Apparatus. A cylindrical cell with an anode compartment separated from a cathode by a glass frit and Hokuto Denko instrumentation (HA-501 Potentiostat, HF-201 Coulombmeter and HB-105 Function Generator) were used for the controlled potential electrolysis as well as the recording of current-potential curves and cyclic voltammograms of the catholyte. The mercury pool with 13.5 cm^2 surface area and a platinum plate were employed as working and counter electrodes, respectively, and the potential of the cathode was referred to SCE. The supporting electrolyte was 0.1 M $[Bu^n{}_4N][BF_4]$. Current-potential curves and cyclic voltammograms were recorded under N_2 or CO_2 with the scan rate of 2 and 200 mV s^{-1}, respectively.

Controlled Potential Electrolysis. A DMF solution containing 2 mM cluster **1** or **4** and 0.1 M $[Bu^n{}_4N][BF_4]$ was electrolyzed under CO_2 until the appropriate electricities passed, using the apparatus described above. CO_2 was continually bubbled through the catholyte (20 ml) during the electrolysis. Change in the cluster concentration with time was followed by recording the cyclic voltammograms of the catholyte directly and by measuring the absorption spectra of small portions of the catholyte diluted 4 times with DMF. Absorption spectra were recorded on a Shimadzu UV-240 spectrometer using a quartz cell with 1.0 mm path length connected to a Schlenk tube.

Analysis of the Product by HPLC. To the electrolyte was added water and then the solid precipitated was removed by filtration, which contains the supporting electrolyte and the compounds originated from clusters. The colorless filtrate was adjusted to 100 ml in volume with water and analyzed directly by Toyo Soda HLC-803 equipped with the column packed with a weakly basic anion exchange resin (Toyo Soda DEAE-2SW). The products were eluted at the flow rate of 0.7 ml min^{-1} by the phosphate buffer solution (pH 5.0) prepared by dissolving KH_2PO_4 (9.87 g) in distilled water/acetonitrile (725 ml/275 ml). To analyze oxalate pH of the eluant had to be neutralized up to 6.6. Chromatograms were recorded on a Toyo Soda UV-8 model II detector by monitoring the absorbance at 200 nm. A typical chromatogram is shown in Fig. 6. The amounts of formate and phenylacetate were determined from the calibration curve plotted separately.

Isolation and Characterization of the Products. As for the products formed by the electrolysis using cluster **1** and cluster **4**, an assignment by HPLC was not successful except for formate. Thus, isolation of four products from the former system (peaks A, C, D, and E in Fig. 6) and two from the latter was carried out. After the addition of water (about 200 ml) to the combined catholyte (about 350 ml) of the repeated electrolyses, the mixture was filtered. The filtrate was evaporated to nearly dryness in vacuo and the residue was extracted with water (100 ml×3). The extracts were combined, concentrated to about 50 ml and then fractionated by preparative HPLC. Since the phosphate buffer solution was used as the eluant, all fractions dried up contained KH_2PO_4 as the main component. So the residues were extracted with appropriate solvent by using Soxhlet extractor and the extracts were dried up carefully. The resulting solid or oil was characterized by recording its

IR and NMR spectra on Shimadzu IR-400 and JEOL GX-400 spectrometers, respectively.

The financial support of this research by the Ministry of Education, Science and Culture of Japan (Grant-in-Aid for Scientific Research 60119001) is greatly appreciated.

References

1) E. Lamy, L. Nadjo, and J. M. Savéant, *J. Electroanal. Chem. Interfacial Electrochem.*, **78**, 403 (1977).
2) L. V. Haynes and D. Sawyer, *Anal. Chem.*, **39**, 332 (1967).
3) J. C. Gressin, D. Michelet, L. Nadjo, and J. M. Saveant, *Nouv. J. Chim.*, **3**, 545 (1979).
4) P. G. Russel, N. Kovac, S. Srinivasan, and M. Steinberg, *J. Electrochem. Soc.*, **124**, 1329 (1977).
5) S. Meshitsuka, M. Ichikawa, and K. Tamaru, *J. Chem. Soc., Chem. Commun.*, **1974**, 158.
6) K. Hiratsuka, H. Sasaki, and S. Toshima, *Chem. Lett.*, **1977**, 1137.
7) K. Takahashi, K. Hiratsuka, H. Sasaki, and S. Toshima, *Chem. Lett.*, **1979**, 305.
8) B. Fisher and R. Eisenberg, *J. Am. Chem. Soc.*, **102**, 7361 (1980).
9) M. Beley, J.-P. Collin, R. Ruppert, and J.-P. Sauvage, *J. Chem. Soc., Chem. Commun.*, **1984**, 1315.
10) J. Hawecker, J.-M. Lehn, and R. Ziessel, *J. Chem. Soc., Chem. Commun.*, **1984**, 328.
11) S. Slater and J. H. Wagenknecht, *J. Am. Chem. Soc.*, **106**, 5367 (1984).
12) B. A. Averill, T. Herskovitz, R. H. Holm, and J. A. Ibers, *J. Am. Chem. Soc.*, **95**, 3524 (1973).
13) M. Tezuka, T. Yajima, A. Tsuchiya, Y. Matsumoto, Y. Uchida, and M. Hidai, *J. Am. Chem. Soc.*, **104**, 6834 (1982).
14) V. Kaiser and E. Heitz, *Ber. Bunsen. Gesell.*, **77**, 818 (1973).
15) J. Cambray, R. W. Lane, A. G. Wedd, R. W. Johnson, and R. H. Holm, *Inorg. Chem.*, **16**, 2565 (1977).
16) G. Christou and C. D. Garner, *J. Chem. Soc., Dalton Trans.*, **1979**, 1093.
17) G. Christou and C. D. Garner, *J. Chem. Soc., Dalton Trans.*, **1980**, 2354.
18) T. E. Wolff, J. M. Berg, K. O. Hodgson, R. B. Frankel, and R. H. Holm, *J. Am. Chem. Soc.*, **101**, 4140 (1979).
19) K. S. Hagen, A. D. Watson, and R. H. Holm, *J. Am. Chem. Soc.*, **105**, 3905 (1983).